Research Article

Ernst Kussul, Tetyana Baydyk*, Alberto Escalante Estrada, Maria Teresa Rodríguez González, and Donald Wunsch II

Solar concentrators manufacture and automation

Abstract: Solar energy is one of the most promising types of renewable energy. Flat facet solar concentrators were proposed to decrease the cost of materials needed for production. They used small flat mirrors for approximation of parabolic dish surface. The first prototype of flat facet solar concentrators was made in Australia in 1982. Later various prototypes of flat facet solar concentrators were proposed. It was shown that the cost of materials for these prototypes is much lower than the material cost of conventional parabolic dish solar concentrators. To obtain the overall low cost of flat facet concentrators it is necessary to develop fully automated technology of manufacturing and assembling processes. Unfortunately, the design of known flat facet concentrators is too complex for automation process. At present we develop the automatic manufacturing and assembling system for flat facet solar concentrators. For this purpose, we propose the design of flat facet solar concentrator that is convenient for automatization. We describe this design in the paper. At present, almost all solar-energy plants in the world occupy specific areas that are not used for agricultural production. This leads to a competition between the solar-energy plants and agriculture production systems. To avoid this competition, it is possible to co-locate solar-energy devices in agricultural fields. The energy obtained via such co-location can be used for agricultural needs (*e.g.*, water extraction for irrigation) and other purposes (*e.g.*, sent to an electrical grid). In this study, we also describe the results of an investigation on co-location methods for the minimal loss of agricultural harvest too.

Keywords: solar concentrator, flat mirror solar concentrator, parabolic dish solar concentrator, automation of manufacturing and assembling process, computational vision, neural networks, co-location, agricultural field

PACS: 89.00, 89.30 cc

*Corresponding Author: Tetyana Baydyk:** Instituto de Ciencias Aplicadas y Tecnología, Universidad Nacional Autónoma de México, Circuito Exterior S/N, Ciudad Universitaria, CP 04510, Ciudad de México, México; Email: t.baydyk@icat.unam.mx

1 Introduction

In this study, we propose the integration of solar devices in agro-ecosystems. This theme has attracted attention from researchers around the world. Preliminary studies in this area have been performed in different countries, such as the United States, Italy, and Spain [1–3].

In [1], three principles are considered for the incorporation of solar devices into agro-ecosystems: 1. the agricultural crops comprising the agro-ecosystem, 2. the solar-energy production, and 3. the integration of the solar devices into the agro-ecosystems. For the first principle, the task is to maximize the biomass production and minimize the changes in the production systems. Energy-production devices are placed in existing fields, and the agricultural production does not change drastically. For the second principle, the task is to maximize the solar-energy output and minimize any changes to the standard technology for acquiring solar energy, thus encouraging agricultural development around renewable-energy facilities. For the third principle, the task is to combine both the aforementioned aspects and gain advantages by increasing the biomass and the power capacity of the solar devices. In this study, we focused on the third approach.

It has been demonstrated that solar energy systems can contribute to agricultural systems via wind-erosion reduction and water conservation.

The first problem that must be solved is the selection of the types of solar concentrators and the agricultural crops that are suitable with these concentrators. Solar-energy requirements vary among crops according to their metabolism (C3 and C4 plants), particularly to the point of light compensation in the phenological stage, in such a

Ernst Kussul: Instituto de Ciencias Aplicadas y Tecnología, Universidad Nacional Autónoma de México, Circuito Exterior S/N, Ciudad Universitaria, CP 04510, Ciudad de México, México
Alberto Escalante Estrada, Maria Teresa Rodrıguez González: Colegio de Postgraduados – Campus Montecillo, Institución de Enseñanza e Investigación en Ciencias Agrícolas, Carretera-Texcoco, km 36, Texcoco, Estado de México
Donald Wunsch II: Electrical and Computer Engineering, Missouri University of Science & Technology, 131 Emerson Electric Co. Hall Rolla, MO 65409-0040

way that the designs of solar concentrators and methods of positioning (distance and altitude of the posts) can generate different percentages of energy yields in accordance with the requirements of the selected crops. The solar concentrator can generate more energy if it has a parabolic-dish form with two axes for sun tracking. This type of solar concentrator can operate in two modes: 1. the mode of capturing the solar energy, where the parabolic dish axis is oriented towards the sun; and 2. the mode of minimum shadow generation, where the axis of the parabolic dish is perpendicularly oriented towards the sun. This permits us to use an optimal strategy for solar-energy generation and thus achieve better crop growth.

On the other hand, each site of the solar concentrator has components that can be used to store rainwater for irrigation and for catching rainfall near or around the posts. The rainwater-capturing device may resemble an inverted umbrella that is opened during rain and closed when there is no rain. The stored water can be used for irrigation using the solar-energy.

Our hypothesis is based on the concept of solar-device placement in areas occupied by agricultural crops, such that the interference between the solar devices and the crops is minimal and thus the solar devices benefit the agricultural crops (Figure 1). We aim to investigate the possibilities of solar-energy device placement in areas occupied by agricultural crops considering the specific conditions of arid and semi-arid regions.
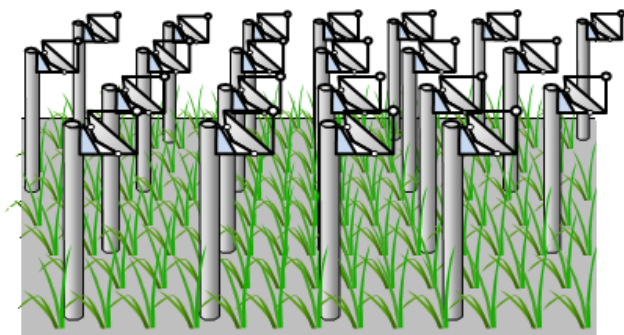

Figure 1: Solar-device placements in areas occupied by agricultural crops

As the first step, on the basis of the literature, we select agricultural crops and solar concentrators to be placed in a given area. The second step involves the design and development of solar concentrator prototypes, as well as their installation in an experimental agricultural field. The third step involves the manufacture of prototypes and the instal-

lation of solar concentrators. The fourth step involves the conduction of experiments for obtaining data regarding the optimal strategy for the placement of the solar hubs in the agricultural crops. The fifth step involves the development of the first version of an optimal strategy for the placement of solar concentrators in agricultural crops. The sixth step involves the development of rainwater-storage prototypes. The last step involves the manufacture of new prototypes with parameters obtained after experimental tests with first prototypes. At present, we are at the first step.

The placement of solar devices in different crops, such as, agave, sunflower, and aloe [3–6] has been investigated previously, but there is a lack of research on crops that are common and popular in Mexico, such as bean, corn, and amaranth. In many studies, solar devices based on flat photovoltaic panels have been analyzed. These panels have a low ratio of the solar energy to the shade area. A higher ratio is achieved by using parabolic dish-type solar devices with two axes for sun tracking. It is interesting to investigate the possibilities of parabolic-dish placement in the crops important for Mexico.

Our research group developed, manufactured, and assembled solar parabolic dishes based on flat mirrors [7, 8]. We began to develop flat-mirror solar concentrators shaped as a parabolic dish. Our work was first published in an international journal in 2008 [9]. On the basis of these developments, we applied for, and obtained seven patents: four in Mexico, one in the United States, and two in Spain [10–16].

Among the important agricultural crops for Mexico, the staple crops of corn (*Zea mays L.*), bean (*Phaseolus vulgaris L.*), and another bean (*Phaseolus coccineus L.*) were selected. They grow with restrictions of the solar-energy intensity and the drought periods. These plants require supports or a trellis for growth, and because of the canopy size, they cast a shadow over everything in the lower tiers, for example, corn-bean [17] and sunflower-bean [18], limiting the growth and cultivation of these lower plants. Under this condition, we can select alternative crops of nutritional interest for production of unsaturated oil, for example, sunflower (*Helianthus annuus L.*) and canola (*Brassica napus L.*). For agriculture that requires irrigation, especially if the water is extracted from the soil via electrical energy, the use of solar prototypes can reduce the cost of the crop production in the agro system. The solar concentrators installed among the crops are appropriate for increasing the rate at which the solar energy is applied to the shaded area of the plants compared with photovoltaic panels. The water stored by the proposed prototypes is important for the further development and quality of the agro system. The farmers can achieve greater income from their

crops, and the deficit of food production in the country can be reduced.

The primary aims of this study are to develop a scheme for the placement of solar concentrators among agricultural crops that are important for Mexico and to develop an optimal strategy for the placement of these solar concentrators in different stages of crop growth. Additionally, we hope to identify the main parameters for the placement of solar concentrators in agricultural areas (for example, the height of posts and distance between posts). Herein, we describe an additional result: a new solar-concentrator design that we developed and manufactured. An additional task is rainwater collection using the same solar concentrator.

Currently, renewable-energy plants are usually placed in exclusive areas selected for this purpose. Government support allows renewable-energy companies to pay a higher income per field than agricultural companies can pay. Thus, renewable energy appears as a competitor of agricultural farms. This situation can be improved by placing solar devices in areas occupied by agricultural crops. The potential impact of this work is the preservation and more efficient usage of land area. Other impacts of the placement of solar concentrators in farmland have been identified. The capture and storage of rainwater is the first impact of the use of solar concentrators at the same sites. Saving rainwater is very important, particularly for crops grown in areas with water-limiting conditions, such as arid and semi-arid areas, as well as for crops grown under "temporary" conditions; *i.e.*, the crop can only be grown during abundant rainfall. In Mexico, approximately 74% of the agricultural production occurs under this condition.

The infrastructure set up for the installation of solar devices allows for the introduction of autonomous robots that use an electric power supply similar to that of trolleybuses. This infrastructure allows the robots to solve navigation problems, giving rise to electrical energy that is cheaper than energy obtained from oil, and can enable the automation of agricultural operations (preparation of the soil, control of pests, etc.).

The development of new solar concentrators and other devices is needed. Section 2 describes the new solar-concentrator design.

2 Solar concentrator

This solar-concentrator design belongs to the area of solar-energy collection and can be used for manufacturing low-cost and low-weight parabolic-dish solar concentrators.

The aforementioned advantages of solar-dish concentrators are achieved via a special manufacturing method using a precision parabolic dish mold with distant stems installed on the convex surface of the mold. This design permits us to approximate the parabolic-dish surface with triangular flat mirrors that are placed with their vertices on the distant stems of the mold.

There are various proposals for fabricating a parabolic-dish solar concentrator from numerous flat mirrors. One such scheme is shown in Figure 2.
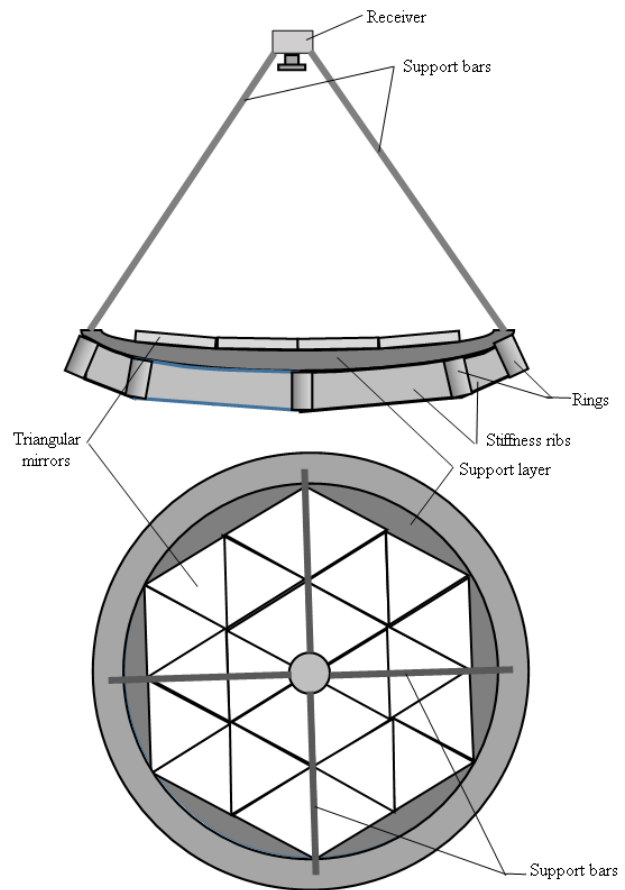

Figure 2: Parabolic-dish solar concentrator with receiver

The solar concentrator contains numerous small, flat triangular mirrors; a parabolic support layer made from a composite material; and stiffness ribs pasted to the rear side of the composite support layer. The stiffness ribs are supported with rings pasted perpendicularly to the rear side of the parabolic composite layer. The solar concentrator contains a receiver for solar energy that is supported by special support bars at the focal distance from the parabolic dish. The receiver can contain a high-concentration photovoltaic cell, a collector for thermal en-

ergy, or both. This chapter describes the design and manufacture of the flat-mirror concentrator. The manufacturing method employs a special mold with a precise convex parabolic surface.

Recently, several methods of mold-based manufacturing for parabolic-dish concentrators have been proposed [19–21]. A large solar concentrator was fabricated at the Australian National University [22]. This concentrator has a parabolic-dish support frame with a surface area of 20 m². It contains approximately 2,300 flat mirrors pasted to the concave side of the support frame. The authors have proposed that the support frame of a flat-mirror solar concentrator be made as a truss structure [21, 23]. Such support frames are expensive, and the precise adjustment of the parabolic-dish surface with the flat mirrors is difficult.

The simplest method for creating a flat-mirror concentrator is to construct a replica of the convex surface of a parabolic dish and paste to this surface numerous flat mirrors that approximate the parabolic shape of the concentrator. A parabolic satellite-television antenna can be used as a mold for the replica creation. The main drawback of this method is the loss of precision of the replica shape after the separation of the replica from the mold. The shape of the concentrator can be corrected after the gluing of the mirrors if the concentrator is clamped to the convex surface of the mold while the glue hardens. In this case, it is possible to obtain a high precision but not the precision of the mold.

Another method that permits us to obtain a concentrator precision almost equal to the precision of the mold is described in [19]. Here, three distant stems of equal height are pasted to the front surface of the flat triangular mirrors at each vertex (Figure 3).
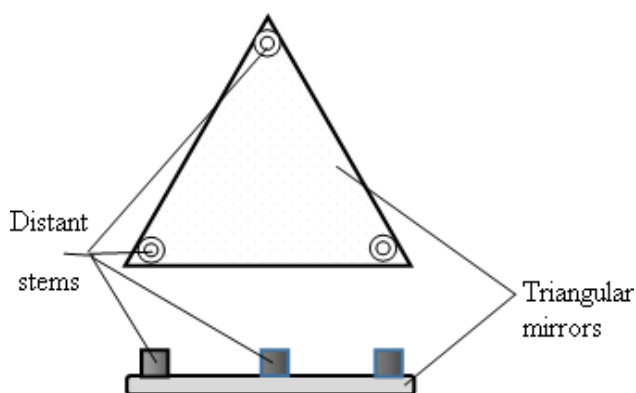

Figure 3: Triangular mirror with three distant stems

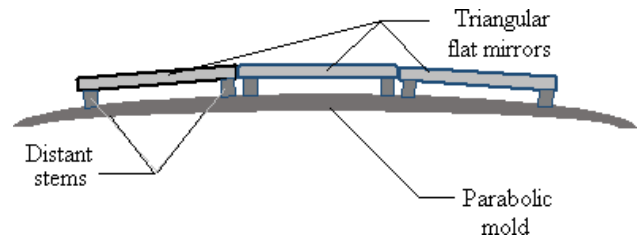The triangular mirrors are installed on the convex surface of the parabolic mold, as shown in Figure 4.

Figure 4: Flat mirrors with distant stems installed on the parabolic-dish mold

Then, flexible strips (of paper, tissue, or fiberglass) are pasted on the back sides of the mirrors using epoxy resin. These strips are pasted in three different directions. After the hardening of the epoxy resin, the strips form a composite support layer for the flat mirrors that approximates the shape of the parabolic dish. Additional stiffness ribs can be glued on the convex part of the support frame if necessary.

The main drawback of this method is the large number of distant stems that must be manufactured for one concentrator. If the concentrator is intended to support a highly concentrated photovoltaic cell with a high concentration, it must contain approximately 2,000 flat triangular mirrors and thus, approximately 6,000 distant stems. This increases the cost of the concentrator. To avoid the high cost, we propose a new method for manufacturing the concentrator.

The main idea of the new method is to place another type of distant stem (mold distant stems) on the convex side of the mold instead of the vertices of the triangular mirrors of the concentrator (Figure 5).
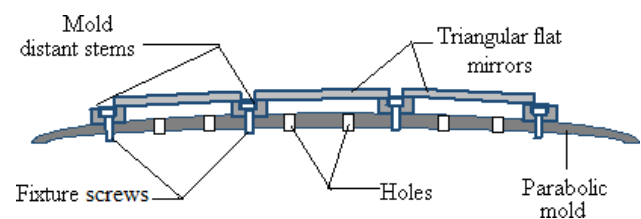

Figure 5: Parabolic-dish mold with distant stems and fixture screws

The mold can be used to assemble many solar concentrators and after the distant stems are manufactured, it is not necessary to repeat the manufacturing process for each new concentrator. The mold distant stems can have a cylindrical shape with a height equal to that of the stems pasted on the triangular mirrors. The diameter of each stem is 2–3 times larger than the diameter of the mirror stem. Each stem is fixed with a fixture screw on the convex side of the mold at the location that corresponds to

the junction of the six vertices of the neighboring mirrors. Therefore, each stem supports six mirror vertices. After the installation of all the mold distant stems, the parabolic surface formed by the outer ends of the stems can be corrected using a computer numeric control machine tool (milling machine tool or lathe). This procedure increases the precision of the mold.

Triangular mirrors are placed on the distant stems (Figure 5). The front surface of each mirror is directed towards the convex mold surface. There are different methods for fixing the positions of the mirrors before the application of the flexible adhesive strips. The simplest method is to use the proper weights of the mirrors. Here, the whole area of the mirrors on the mold is outlined with special borders that are fixed to the convex surface of the mold. The mirrors are placed densely so that their borders touch, and they cannot change places after filling the entire area. Another method is to put glue on the borders of on the mirrors (approximately at the center of each border) in order to connect the mirrors in the process of their co-location. This method is less vulnerable to occasional movements of the mold that occur during assembly. Micro grooves can be formed on the borders of the mirrors to increase the strength of the glued connections. The third method employs an air flow that clamps mirrors to the distant stems. This air flow is created by a suction ventilator placed under the mold. The air pressure under the mirrors is low because of the holes in the mold. The third method provides better possibilities for clamping the mirrors to the mold during the hardening of the resin, increasing the precision. This method can be used jointly with the second one. An alternative method for clamping the mirrors to the mold is to use a sheet of elastic tissue for covering the mirrors during the hardening of the composite.

To create the composite layer on the back sides of the mirrors (Figure 6), different materials can be used.

The flexible strips can be made from paper, synthetic or natural tissues, fiberglass tissue, etc. While paper is the cheapest solution, paper-based composites tend to change shape under humidity. Fiberglass-tissue composites provide the best stability and rigidity but are expensive. To fill the composites, different polymer resins can be used. Epoxy resin has attractive properties, such as low creep during hardening, a high working temperature, and good adhesion; however, it is expensive. Cheaper resins can be used if the precision of the concentrator is not important.

The composite layer (Figure 2) is formed by successively pasting flexible strips in the three main directions of the concentrator. As a general rule, the width of the strip should cover one line of the triangular mirrors (Figure 6).
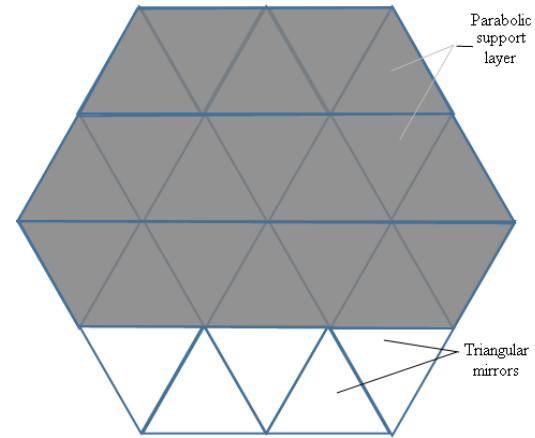

Figure 6: Paper or fiberglass strips pasted to the rear side of triangular mirrors
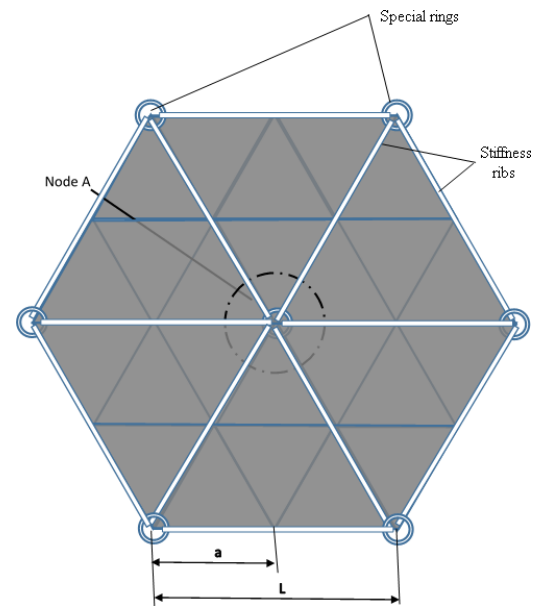

Figure 7: Rear side of solar concentrator. An example of stiffness-rib co-location. a is the triangular-mirror size, and L is the stiffness rib length
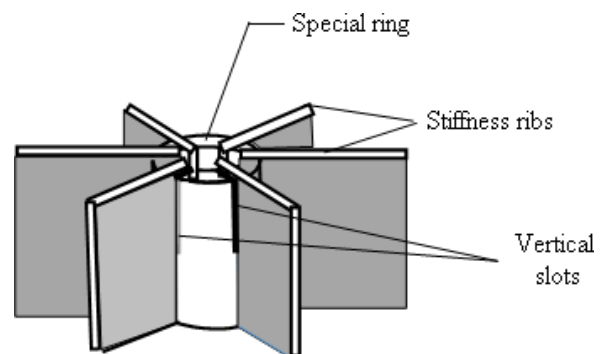

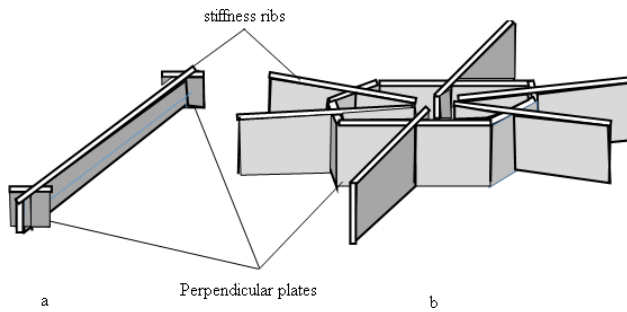**Figure 8:** Node A; connection of stiffness ribs

Figure 9: Stiffness ribs: a) a stiffness rib and b) a schematic of the stiffness-ribs connection

However, it is possible to use slightly wider strips, yielding overlap, or to use slightly narrower strips, yielding gaps.

If the rigidity of the concentrator requires improvement after the hardening of the composite layer, additional stiffness ribs (Figure 7) can be installed on the back side of the composite layer.

One method for stiffness-rib co-location is shown in Figure 7. Here, special rings are pasted at the locations where the vertices of the neighboring mirrors are jointed. The axis of each ring is perpendicular to the composite layer. The ring contains vertical slots for connecting the stiffness ribs (Figure 8).

All the stiffness ribs are glued to the composite layer and to the vertical rings. In Figure 7, the length of the stiffness rib L and the length of the mirror side a are shown. The relationship between these values is given by the following equation:

$$L = n * a, \quad \text{where } n = 1, 2, 3, \dots \tag{1}$$

When $n > 1$, not all the joints of the vertices contain connection rings (Figure 7). Different designs can be used for connecting the stiffness ribs. One such design is shown in Figure 8. Here, the connection ring has the shape of a hollow tube with six slots in the upper end. Each stiffness rib has two lugs that can be introduced to the slot of the two rings and pasted there during the concentrator assembly. The stiffness rib is glued to the rear surface of the composite layer.

Another design for the connection of the stiffness ribs is shown in Figure 9.

In this case, each stiffness rib has two perpendicular plates pasted to the rib near its terminals (Figure 9, a). Six neighboring stiffness ribs are installed in such a manner, such that all the perpendicular plates touch each other and are glued to each other (Figure 9, b). Together, the plates form a hexagonal ring that serves as a support device for the stiffness ribs. As in the previous case, the stiff-

ness ribs are glued to the rear surface of the composite layer.

This solar concentrator contains a solar receiver (Figure 10) that collects solar energy. Different devices can be used for this purpose. One version of the solar receiver is shown in Figure 11. This receiver collects thermal energy that can be used directly for heating or can be supplied to heat engines to generate electricity. The receiver contains a support plate (Figure 11), a focal-position adjustment device, a base plate, and a thermal energy collector.

If the parabolic-dish concentrator is manufactured with precision, the shape of the focal light spot is a six-pointed star (Figure 10). Thus, the shape of the thermal-energy collector is also a six-pointed star. This is ideal for heating applications but is not optimal for electricity generation, because the efficiency of the thermal solar electricity generator is lower than the efficiency of the concentrating photovoltaic cells.

In another type of receiver (Figure 11), a high-concentration semiconductor solar cell is installed in the most illuminated area (Figure 11) of the receiver.

The illumination in the most illuminated area is twice as high as that in the less illuminated area. High-concentration solar cells require equal distribution of the illumination throughout the active area; thus, it is worthwhile to place the semiconductor chip in the highly illuminated area, as shown in Figure 11. It is also useful to use a
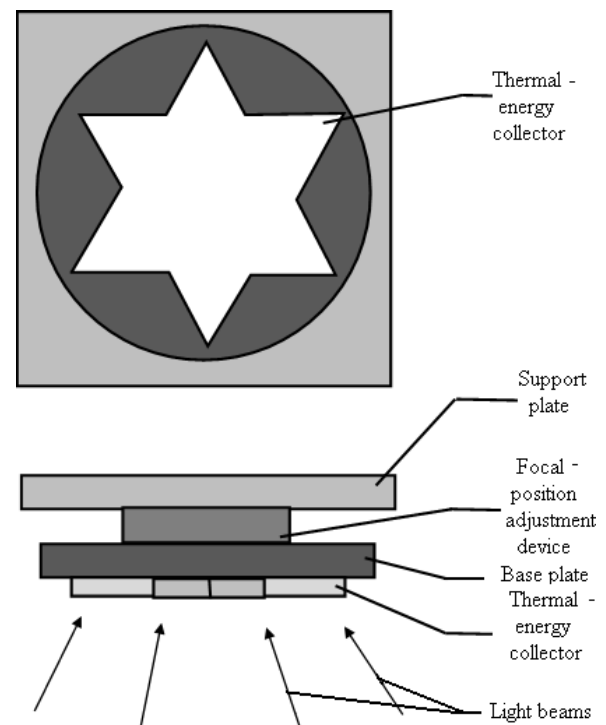

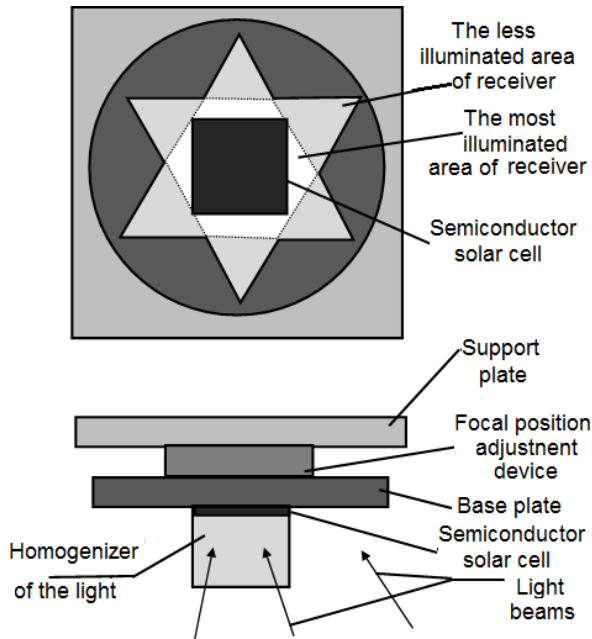**Figure 10:** Thermal-energy receiver
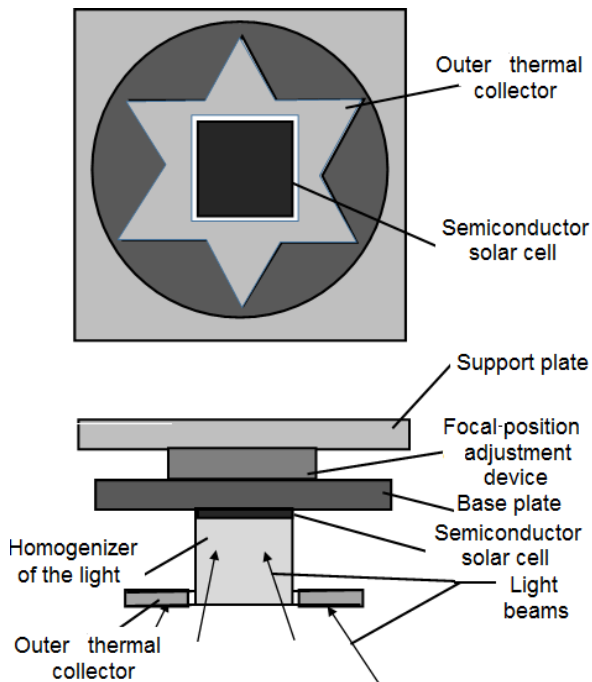
Figure 11: Photovoltaic receiver

Figure 12: Combined photovoltaic and thermal-energy receiver

homogenizer for the light, which can be implemented as a glass prism or a well from the mirrors. The entering solar beams are shown in Figure 11.

The disadvantage of this type of receiver is the large portion of concentrated light (the most illuminated area and the less illuminated area) that is not used for energy

generation. To avoid this drawback, we present a third type of concentrator, as shown in Figure 12.

This concentrator contains a high-concentration semiconductor solar cell at the center of the base plate, a light homogenizer, and an outer thermal collector that has the shape of a six-pointed star and is located around the homogenizer (Figure 12). The high-concentration semiconductor solar cell transforms solar energy from the highly illuminated central area with a high efficiency. The remaining solar energy can be used for heating or electricity generation with a moderate efficiency.

3 Automatic assembly system

In this work we use the results of our previous investigations [24, 25]. The scheme of automatic assembly system is presented in Figure 13.
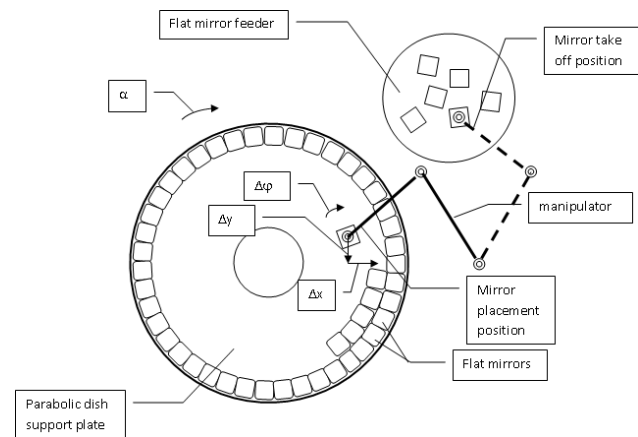

Figure 13: Automatic assembly system

It contains parabolic dish support plate that can rotate around the central point with precision of 0.1 mm for external circle. It rotates with stepping micro motor developed for our micro equipment technology (MET) [26]. The system has a micro manipulator that takes the flat mirrors from the feeder, moves it to the mirror placement position, orientate it, and place it on the corresponding position in support plate. All these operations are made under the control of computer vision system. For this purpose, two cameras are placed over the assembly devices (the cameras are not shown in Figure 13). The first camera is placed over the mirror take off position. The second camera is located over the mirror placement position. The system works as follows:

- computer vision system searches for flat mirror that can be taken from the feeder. For this purpose, the first camera is used;
- manipulator transfers the mirror to the mirror placement position;
- in this position of manipulator the computer vision system calculates three variables: $\Delta\phi$ - the rotation angle of flat mirror needed to obtain correct orientation of this mirror, Δy- the displacement in y direction needed to get correct mirror position on the support plate, Δx- the corresponding displacement in x direction;
- manipulator makes needed movements, put down the mirror and glues it;
- after that the support plate is rotated to free placement position for the next flat mirror.

Recently, we made several investigations similar to described in this system. We adapt them for the system to be developed.

To implement the take off procedure it is necessary to recognize the object and its position. So, we have two tasks: object recognition and definition of its position. In our investigations we applied the Random Threshold Classifier (RTC); Limited Receptive Classifier (LIRA) or Permutation Coding Neural Classifier (PCNC) neural classifiers [27].

The described automation focuses on the construction of the reflective surface. We suppose that: the facet support is previously constructed with the parabolic shape, and the triangular mirrors are in a container [28] (Figure 14).
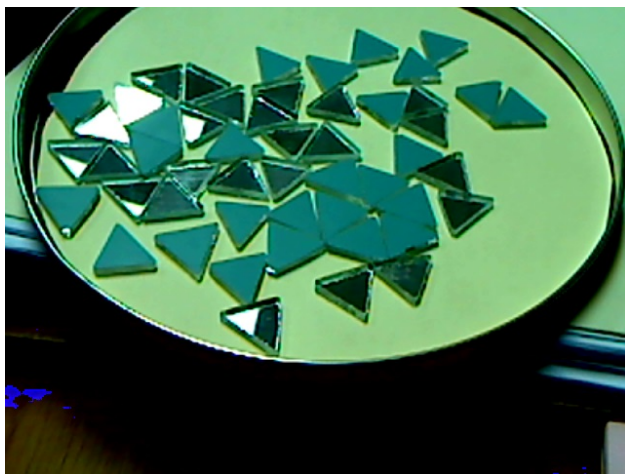

Figure 14: Mirror container

The automation that we describe in this work consists of a computer vision system, which can detect the positions of the mirrors in the container to enable a positioning

system to take the mirrors and individually place them on the correct places over the mirror support.

Computer vision systems share a common structure, which is composed of: a webcam, which transforms images into a digital representation; a pre-processing stage, where we obtain the edges, brightness, contrast or any other important characteristic of images; a classifier, which processes the previously pre-processed information and is an artificial neural network in this case; classes of interest, which are the output of the classifier (Figure 15). We expect to obtain four classes: background, edges, mirror and flip side mirror; or only two classes: background and mirrors. From these classes, we can calculate the mirror center.

Figure 15: Structure of the computer vision system

This computer vision system can be used by a robot-manipulator to take one mirror at each moment. We think that this manipulator can have an inlet or air intake. The mirror can adhere by suction to the manipulator and can be transported to the support frame of the solar concentrator. In this study, we will describe the RTC structure.

The proposed neural classifier is a random threshold classifier (RTC). The RTC is an artificial neural network that has been successfully used to recognize metal textures. Three texture types (Figure 16) were used, and the recognition rate of 79.9% was obtained [29]. The RSC (random subspace classifier), which is a version of the RTC, was used.

These results were significantly improved up to 99.8% using the LIRA (Limited Receptive Area) neural classifier [30].

Now, we will explain the structure of the RTC, which is shown in Figure 17.

The RTC consists of S blocks, each of which has as an input with n features (X_1, X_2, ..., X_n) and an output, which is a neuron (b). Every feature X_i is an input of a pair of neurons: h_i and l_i. h and l are neuron thresholds, *i.e.*, these neurons have one input and one output. The output of the l and h neurons is 1 if the input value is more than the threshold level and 0 otherwise. The threshold values of these neurons are randomly selected, and one condition must be satisfied: threshold l must be less than threshold h. The output of every pair of threshold neurons is connected to an a neuron. l is connected with the excitatory input,
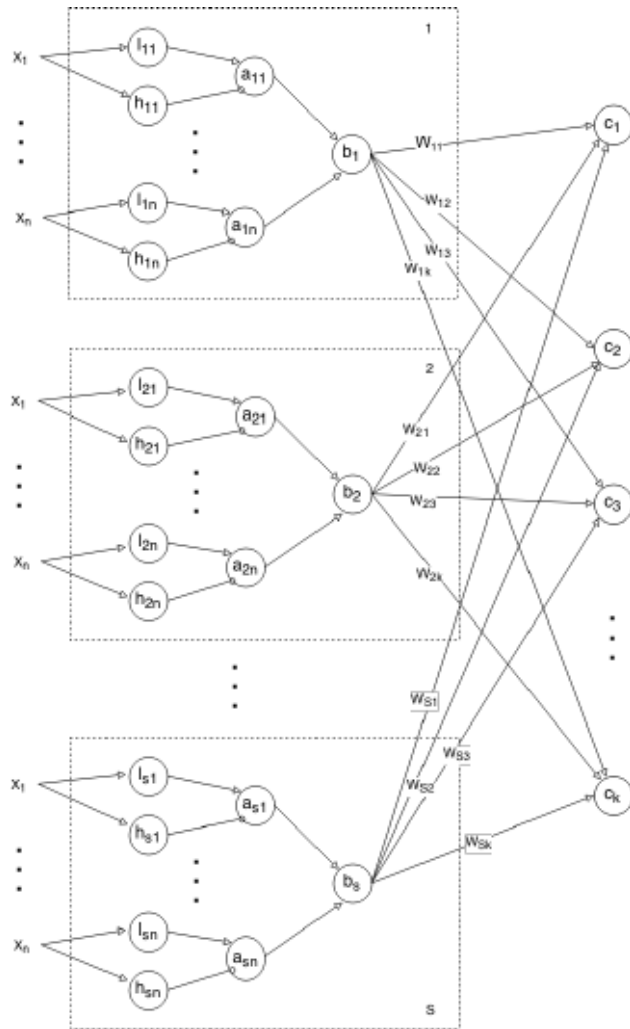
Figure 16: Texture examples

Figure 17: Structure of the random threshold classifier (RTC)

Figure 18: Underlined edges of mirrors for the training

and h is connected with the inhibitory input. Because of these connections, the output of a neuron is 1 only if the input value of the feature is between the threshold levels l and h. The output of every a neuron in each block is connected with the inputs of b neuron. The output of b neuron is 1 only if all inputs are 1. Finally, the outputs of the b neu-
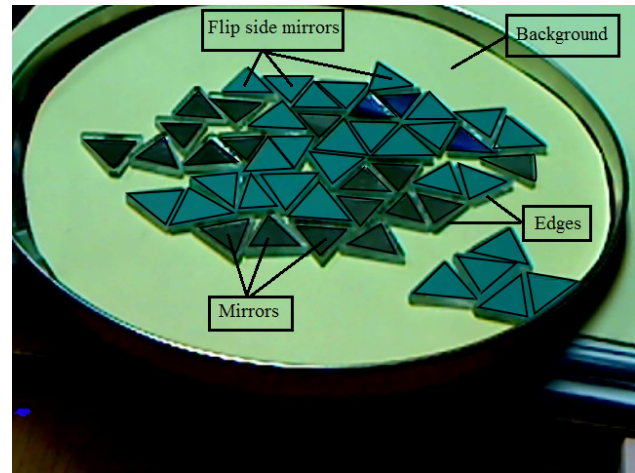
rons are connected with trainable connections to all inputs of the output layer. The output layer is formed by classes to be detected.

The inputs of the RTC (X_1, X_2, ..., X_n) are histograms of brightness, contrast and orientation of previously detected contours. The artificial neural network must be trained to detect the desired objects and features. The image sets are prepared for the training and recognition stages. The images of a set contain triangular mirrors in the container. To train the classifier to detect the edges, a training dataset is prepared, where the edges of the triangular mirrors are underlined, as shown in Figure 18. These marked images are presented to RTC, and for every image, RTC must adjust the weights of the trainable connections. The training stage finishes when we have a local minimum of errors or after a definite number of training cycles.

When RTC recognizes the mirror in the image, we can calculate its coordinates and center of mirror for the manipulator.

If we have the position of the points that conform a mirror, the center can be calculated using a general equation

of a figure with n points at positions x_i:

$$\overline{x} = \frac{\sum\limits_{i=1}^{n} x_i}{n} \qquad (2)$$

If we have the corners, this equation can be simplified, and the center triangle is easily calculated with the corner coordinates (x_i, y_i) as follows:

$$c = \left(\frac{x_1 + x_2 + x_3}{3}, \frac{y_1 + y_2 + y_3}{3} \right) \qquad (3)$$

There are two cases to consider for the calculation: 1) the centers of all triangles were detected, and one was selected; or 2) we calculated the center of the first mirror that the system detected. The first case implies more calculation but can make the classification easier if we have more information. The second case implies less calculation; however, because the manipulator takes the mirrors individually, and the position of the mirrors may change, this method is simpler.

4 Conclusion

Co-location of solar-energy devices in agriculture fields permits us to improve land use and to obtain solar energy and agriculture crops from the same terrain. To obtain the maximum advantages from such a co-location, it is necessary to select agricultural cultivars that are resistant to reduced illumination and to develop solar-energy devices that generate a minimum shadow area and produce the maximum amount of solar energy. Such devices can be made using solar-energy concentrators that can provide an energy output with a value that is 30–40% of the total solar energy. Additionally, the posts that support the solar concentrators can be used for devices that collect rainwater in arid and semi-arid regions. The flat-panel photovoltaic provides advantages for rainwater-collection devices because the large surface area is effective for collecting rainwater.

Parabolic dish solar concentrators have many advantages in solar thermal power plant creation, but usually they have elevated cost, especially when they use shaped mirrors. It is possible to decrease this cost using small flat mirrors (facets) to approximate parabolic dish surface. In this case the cost of materials mainly depends on the size of parabolic dish concentrator. If the size if the dish has the order of magnitude of several meters the cost of materials is slightly less than the cost of the shaped mirrors, but is elevated indeed (for example, 50 USD per square meter). For additional decreasing of material cost it is possible to scale

down parabolic dish concentrators. If the diameter of concentrator is decreased till 0.5 m the material cost may decrease down to 5 USD per square meter, but the labor cost during the scaling down grows very fast. To decrease the labor cost, we need to automate this process. At present we develop the automaton system based on computer vision technology.

We proposed a new method based on neural networks for mirror detection in images. We use a supervised extreme training for our neural classifier. We described the structure and method of the RTC neural classifier that was previously used for metal texture recognition. The problem of mirror recognition is presented as a texture recognition task. In the metal texture recognitions, we obtained a recognition rate of almost 80%. In our task from 89% till 95% of correct recognition was obtained.

The strong lightweight material for facet support frame is developed. This material can be used for other constructions as well.

References

[1] Macknick J., Beatty B., and Hill G., Overview of opportunities for co-location of solar energy technologies and vegetation, Tech. Rep. National Renewable Energy Lab. NREL/TP-6A20-60240, 2013, 18.

[2] Macknick J., Overview of opportunities for co-location of agriculture and solar PV, Clean Energy Econ. Conf., Utica, USA, June 16 2016, 21.

[3] Strom D., Noble M., Davis R., Macknick J., Co-location of agriculture and solar PV, 2013, https://www.eanvt.org/wp-content/uploads/2013/01/NREL-Solar_Pollinators.compressed.pdf.

[4] Transparent solar PV installation among the trees, Trina Solar, 2019, http://www.trinasolar.com/us/resources/downloads.

[5] Shemkus S., Agrivoltaics: solar panels on farms could be a win-win, 2019, https://civileats.com/2019/01/22/agrivoltaics-solar-panels-on-farms-could-be-a-win-win/

[6] Ravi S., Macknick J., Lobel D., Field C., Ganesan K., Jain R., et al., Collocation opportunities for large solar infrastructures and agriculture in dry lands, Appl. Energy, 2016, 165, 383-392.

[7] Kussul E., Baidyk T., Makeyev O., Lara-Rosano F., Saniger J. M., Bruce N., Development of micro mirror solar concentrator, the 2-nd IASME/WSEAS Int. Conf. Energy and Environ. (EE'07), Portoroz (Portorose), Slovenia, May 2007, 294-299.

[8] Kussul E., Baidyk T., Lara-Rosano F., Saniger J. M., Bruce N., Support frame for micro facet solar concentrator, the 2-nd IASME/WSEAS Int. Conf. Energy and Environ. (EE'07), Portoroz (Portorose), Slovenia, May 2007, 300-304.

[9] Kussul, E., Baidyk, T., Lara, F., Saniger, J., Bruce, N., Estrada, C., Micro facet solar concentrator, Int. J. Sustainable Energy, 2008,

27(2), 61-71,

[10] Kussul E., Baidyk T., Lara-Rosano F., Saniger Blesa J.M., Bruce N., Concentrador solar, Abril 2013 IMPI, Mexico, Patente No 309274 (in Spanish).

[11] Kussul E., Baidyk T., Lara-Rosano F., Saniger Blesa J.M., Ascanio G., Bruce N., Method and device for mirrors position adjustment of a solar concentrator, January 2014, U.S. patent 8,631,995 B2.

[12] Kussul E., Baidyk T., Lara-Rosano F., Saniger Blesa J. M., Ascanio G., Bruce N., Método y dispositivo de ajuste de posición de espejos de un concentrador solar, marzo de 2014, IMPI, Mexico, Patente No 313963 (in Spanish).

[13] Kussul E., Baidyk T., Rodríguez Mendoza J.L, Bruce Davidson N.Ch., Saniger Blesa J.M., Lara Rosano F., Sistema automático para ajuste de la superficie parabólica de concentrador solar de espejos planos, agosto 2015, IMPI, Patente No 33260 (in Spanish).

[14] Kussul E., Baidyk T., Saniger Blesa J.M., Bruce Davidson N., Lara Rosano F., Rodríguez Mendoza J.L., Dispositivo de soporte para concentrador solar con espejos planos, octubre 2015, IMPI, Mexico, Patente No 334742 (in Spanish).

[15] Kussul E., Baidyk T., Rodríguez Mendoza J.L., Bruce Davidson N., Saniger Blesa J., Lara Rosano F., Sistema automático para ajuste de la superficie parabólica de concentrador solar de espejos planos, septiembre 2015, Oficina Española de Patentes y Marca, Patente ES2525303 (in Spanish).

[16] Kussul E., Baidyk T., Saniger Blesa J., Bruce Davidson N., Lara Rosano F., Rodríguez Mendoza J.L., Dispositivo de soporte para concentrador solar con espejos planos, septiembre 2015, Oficina Española de Patentes y Marca, Patente ES2525276 (in Spanish).

[17] Delgado Martínez R., Escalante Estrada J.A.S., Díaz Ruíz R., Trinidad Santos A., Morales Rosales E.J., Sosa Montes E., Defoliación en maíz y su efecto sobre el rendimiento de frijol-maíz en asociación, Rev. Mex. de Cienc. Agrícolas, 2014, 5 (6), 1015-1027 (in Spanish).

[18] Escalante-Estrada J.A.S., Rodríguez-González M.T., Escalante-Estrada Y.I., Rendimiento del girasol en función del cultivar de frijol en siembra asociada, Cienc. Agricolas Informa, 2014, 23(1), 23-28 (in Spanish).

[19] Baydyk T., Kussul E., Robles Roldan M.A., New approach to design of flat facet solar concentrators, ICCE 2016, Montreal, Canada, August 2016, 1-7.

[20] Kussul E., Baydyk T., Robles Roldan M.A. New design of flat facet solar concentrators, ICCE 2016, Montreal, Canada, August 2016, 136-147.

[21] Kussul E., Baidyk T., Makeyev O., Lara-Rosano F., Saniger J.M., Bruce N., Development of micro mirror solar concentrator, WSEAS Trans. Power Syst., 2007, 2(8), 188-194.

[22] Johnston G., Focal region measurements of the 20 m2 tiled dish at the Australian National University, Sol. Energy, 1998, 63(2), 117-124.

[23] D.E. Wood, October 1979, Apparatus for supporting large-dimension curved reflectors, U.S. patent 4,171,876.

[24] Toledo-Ramírez G.K., Kussul E., Baidyk T., Neural classifier for micro work pieces recognition, Image Vision Comput., 2006, 24(8), 827-836.

[25] Baidyk T., Kussul E., Makeyev O., Caballero A., Ruiz L., Carrera G., et al., Flat image recognition in the process of microdevice assembly, Pattern Recognit. Lett., 2004, 25(1) 107-118.

[26] Kussul E., Baidyk T., Ruiz-Huerta L., Caballero A., Velasco G., Kasatkina L., Development of micromachine tool prototypes for microfactories, J. of Micromech. Microeng., 2002, 12, 795-813.

[27] Baydyk T., Kussul E., Toledo-Ramirez G.H., Investigation of neural classifiers for recognition of micro components of solar concentrators, Int. J. Mech. Eng., 2017, 2, 19-27.

[28] Robles Roldan M.A., Baydyk T., Kussul E., Desarrollo de software para reconocimiento de imágenes basado en redes neuronales, 4to Congreso Int. Investigación e Innovación en Ing. de Software 2016, CONISOFT 2016, Puebla, Mexico, abril 2016, 119-125 (in Spanish).

[29] Baidyk T., Kussul E., Makeyev O., Texture recognition with random subspace neural classifier, WSEAS Trans. Circuits Syst., April 2005, 4(4), 319-325.

[30] Makeyev O., Sazonov E., Baidyk T., Martin A., Limited receptive area neural classifier for texture recognition of mechanically treated metal surfaces, Neurocomputing, March 2008, 71 (7-9), 1413-1421.